

---

# Lagrangian modeling and properties of particles with inertia

F. Toschi<sup>1</sup>, L. Biferale<sup>2</sup>, E. Calzavarini<sup>3</sup>, E. Lévêque<sup>3</sup>, A. Scagliarini<sup>2</sup>

<sup>1</sup> Department of Physics and Department of Mathematics and Computer Science, Eindhoven University of Technology P.O. Box 513, 5600 MB Eindhoven, The Netherlands

<sup>2</sup> Dept. Physics and INFN, University of Rome, Tor Vergata, Via della Ricerca Scientifica 1, 00133 Rome, Italy

<sup>3</sup> Laboratoire de Physique, École Normale Supérieure de Lyon, CNRS UMR5672, 46 Allée d'Italie, 69007 Lyon, France.

federico.toschi at tue.nl

**Summary.** Recently many efforts have been devoted to the experimental investigations of the Lagrangian properties of particles in turbulence. Different experimental techniques allow to investigate particles with different physical properties, e.g. values of size and density, within some specific range. No experimental studies have been able to cover large range of parameters space. We have recently performed a set of Direct Numerical Simulation (DNS) with the precise goal to cover systematically particles from heavy ones to very light ones. We also performed numerical simulations of particles with the same physical properties at different Reynolds numbers and with different physical modeling. We discuss briefly the limitations of the point particle model and suggest a simple but effective way to extend it.

The transport of particulate by means of turbulent flows is an ubiquitous phenomenon in nature and in industrial applications alike. Turbulent flows are characterised by strong fluctuations both in space and in time of the energy dissipation field, a phenomenon known as intermittency [1].

Here we present results from recent Direct Numerical Simulation (DNS) devoted at investigating the statistical properties of particles in homogeneous and isotropic turbulence. The incompressible fluid velocity  $\mathbf{u}$  are evolved according to the Navier-Stokes equations:

$$\frac{D\mathbf{u}}{Dt} \equiv \frac{\partial\mathbf{u}}{\partial t} + \mathbf{u} \cdot \nabla\mathbf{u} = -\nabla p + \nu\Delta\mathbf{u} + \mathbf{f}. \quad (1)$$

where  $p$  is the pressure and  $\mathbf{f}$  an external forcing injecting energy at a rate  $\epsilon = \langle \mathbf{u} \cdot \mathbf{f} \rangle$ . Equation (1) is integrated numerically by means of a pseudo-spectral code with a second order Adams-Bashforth scheme. The same scheme was also used for the particles evolving according to the dynamic given by

equation (2), where we used tri-linear interpolation to obtain the Eulerian values of the velocity field at the particle's positions (see [2, 3] for details). The forcing applied to the system was chosen to maintain constant the spectral energy content of the first two shells in Fourier space.

The main aim of this set of numerical investigations was to systematically explore the properties of particles at changing the inertia properties. To this end we decided to compromise space (Eulerian) resolution in favour of a larger number of particles classes.

Along with the Eulerian field, the Lagrangian evolution of particles was integrated by means of one of the simplest, yet nontrivial, model for passively advected particles as derived in Refs. [4, 15] which is valid for dilute suspensions of small spherical particles:

$$\frac{d\mathbf{x}}{dt} = \mathbf{v}, \quad \frac{d\mathbf{v}}{dt} = \beta \frac{D\mathbf{u}}{Dt} + \frac{1}{\tau_p}(\mathbf{u} - \mathbf{v}), \quad (2)$$

In the above equations  $\mathbf{x}(t)$  and  $\mathbf{v}(t)$  denote the particle position and velocity, respectively. The parameters in equation (2) are the particle's response time  $\tau_p = a^2/3\beta\nu$  (where  $a$  is the particle radius and  $\nu$  is the viscosity) and  $\beta$  which is related to the density contrast between the density of the particle,  $\rho_p$ , and the one of the fluid,  $\rho_f$ :  $\beta = 3\rho_f/(\rho_f + 2\rho_p)$ . The dimensionless ratio between the response time of particles and the smallest time scale in turbulence (dissipative time scale) is the Stokes number  $St = \tau_p/\tau_\eta$ .

The physical parameters  $St$  and  $\beta$  characterize the particle's properties and it has to be noted that they implicitly carry a dependence from the particle's radius. In the case of particles much smaller than the dissipative scale of turbulence one can treat them as pointwise. The Eulerian flow is characterized by the Reynolds number  $Re$ . The ratio between the particle diameter  $D$  and the dissipative scale of the Eulerian flow may or may not be small, according to the particular value of the parameter  $\beta$ ,  $St$  and  $Re$ . In the case that the ratio  $D/\eta$  is order unity or larger, the physical description in terms of pointwise particles clearly cannot be correct. It is however very difficult to estimate quantitatively the error committed by using the point particle (PP) description as a function of the position in the parameter space. To quantify the importance of the full description of the particle size, we performed recently some numerical simulations where the finite particle size was implemented by means of a coarse graining of the Eulerian velocity field.

We performed four numerical simulations, at resolutions  $128^3$  and  $512^3$  (corresponding to  $Re_\lambda \simeq 75$  and  $Re_\lambda \simeq 180$ ) with point particle model (PP) [6] and with Faxén corrections (FC, see Section 2). The different classes of particles in the  $\beta, St$  parameter space that we studied are reported pictorially in Figure 1. We proceed now to briefly discuss the changes in the phenomenology when one moves from the heavy pointwise particle model, to inertial particles with generic densities and then to particles with finite size.

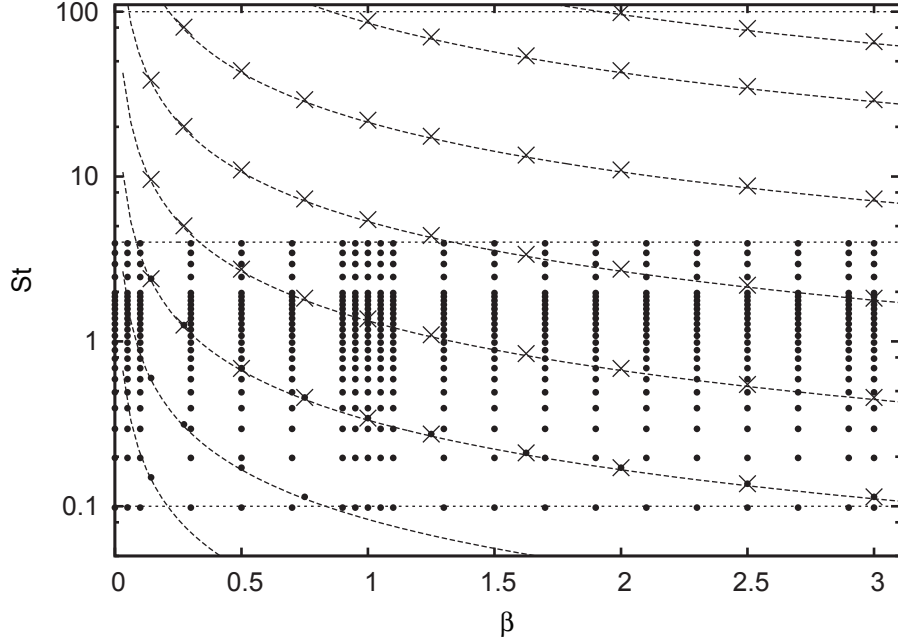


**Fig. 1.** Different class of particles studied in the parameter space,  $(\beta, St)$ . Black dots corresponds to the particles classes integrated at a resolution  $128^3$  with  $Re_\lambda = 75$  and Point Particle model (PP). Crosses corresponds to  $128^3$  ( $Re_\lambda = 75$ ) and  $512^3$  ( $Re_\lambda = 180$ ) for the Faxén corrected (FC) model, see Section 2.

## 1 Lagrangian structure functions

Recently temporal correlations of Lagrangian velocities have been studied by means of Lagrangian Velocity Structure Functions (LVSF) of the particle velocities,  $S^{(p)}(\tau)$ :

$$S^{(p)}(\tau) = \langle |v(t + \tau) - v(t)|^p \rangle \quad (3)$$

where  $v$  denotes one particular component of the particle velocity.

From the structure functions one can readily define what has been dubbed as local slopes, or local scaling exponents:

$$\zeta(p, \tau) = \frac{d \log S^{(p)}(\tau)}{d \log S^{(2)}(\tau)}$$

probably the most sensitive tool to study the presence of eventual homogeneous scaling in the inertial range and to quantify associated uncertainties. It was shown that the local slopes of the LVSF do present a strong dip at scales intermediate between the dissipative scales and the inertial range [8, 9]. The dip is present in all currently available datasets (both experimental and

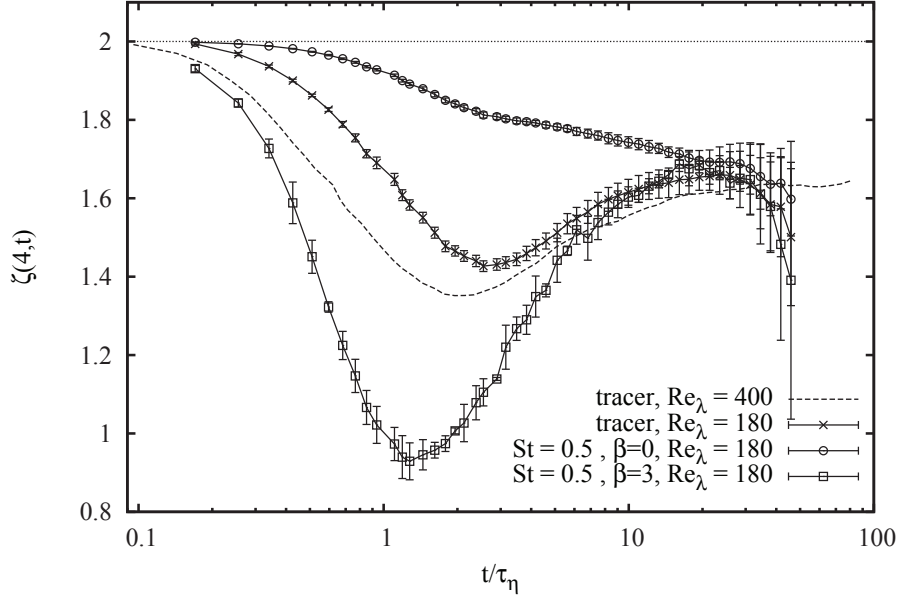


**Fig. 2.** Relative local slopes of  $\zeta(4, \tau)$  vs.  $\zeta(2, \tau)$  of LVSF for: tracers at  $Re_\lambda = 400$  (solid line); tracers at  $Re_\lambda = 200$  (red squared); heavy particles with ( $St = 0.5$ ,  $\beta = 0$ ) (green circles) and light particles with ( $St = 0.5$ ,  $\beta = 3$ ) (blue triangles). Notice the small enhancement on the dip for tracers at increasing Reynolds and the big enhancement/depletion for light/heavy particles respectively. Both trends confirm the importance of velocity statistics associated to small scale vortical filamentary structures in the dip region.

numerical ones) [10]. It has also been shown that the dip can be explained in terms of a multifractal modeling [10] of Lagrangian velocity increments and that it is suppressed either by filtering the velocity signal or by observing heavy particles instead of passive tracers [11]. This last observation leads to the conclusion that the dip is mainly sensitive to the statistics of small scale vortex filaments.

Here we show for the first time the behaviour of the local slopes for tracers, heavy and light particles evolving in the same turbulent flow. As it can be seen from Figure 2 the dip in the case of light particles is even more strongly pronounced. It is well known that light particles tends to accumulate in small scale vortex filaments [12], this is another strong evidence of the fact that the dip is strongly sensitive to the statistical fluctuations of the velocity field around small scales vortex filaments. In Figure 2 one may also notice a small enhancement of intermittency (i.e. on the dip excursion) at

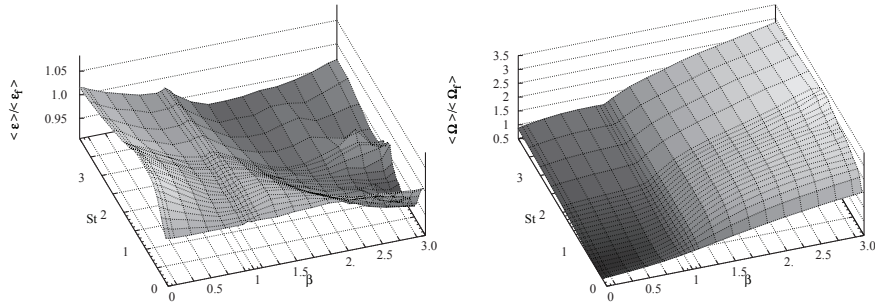


**Fig. 3.** The average energy dissipation of the fluid (left) and mean enstrophy (right) at the position of the particles normalized by the averaged values for fluid tracers, as a function of different particles properties ( $\beta$ ,  $St$ ).

increasing Reynolds for the tracers statistics, indicating a possible non trivial dependency of the vortex filament statistics on Reynolds number.

Another statistical quantity useful to quantitatively measure the preferential concentration for light particles in high vorticity regions is visible in Figure 3, where it is shown the energy dissipation field,  $\varepsilon = \sum_{i,j} (\partial_i u_j + \partial_j u_i)^2$ , and the enstrophy (squared vorticity) magnitude,  $\Omega = \sum_{i,j} (\partial_i u_j - \partial_j u_i)^2$ , calculated at the particle positions for all  $\beta$  and  $St$ . As one can see, light particles have a pretty larger total vorticity when normalized with the corresponding value measured on the tracers (up to a factor 3).

## 2 Finite particle size

The point particle model is computationally efficient, theoretically simple and often an excellent approximation of physical reality. On the other hand, is to be expected that larger particles can behave in a considerable different way from material points and that to describe them the PP model cannot be employed.

In [13] it is described how to model finite size particles by adding to the equation for the particles motion the Faxén terms which account for the non-uniformity of the flow at the particle-scale. Faxén forces represent corrections for particles in turbulence with dimension  $D > \eta$ . We chose to model finite size particles in this way, in order to maintain a good computational efficiency. Indeed the finite size correction only implies some extra Fourier Transform and, once implemented, many particles can be integrated with essentially no additional computational costs. Adding an extra class of particle (diameter) do instead imply an additional computational cost. The Faxén theorem for the drag force on a moving sphere states that:

$$\mathbf{f}_D = 6\pi\nu\rho_f a \left( \frac{1}{4\pi a^2} \int_{S_a} \mathbf{u}(\mathbf{x}) dS - \mathbf{v} \right) = 6\pi\nu\rho_f a (\langle \mathbf{u} \rangle_{S_a} - \mathbf{v}), \quad (4)$$

with the integral evaluated over the surface of the sphere and where  $\mathbf{u}(\mathbf{x})$  is the non homogeneous velocity of the fluid in the absence of the sphere. As shown in [15] also Faxén forces via sphere volume average must be included. The expression for the fluid acceleration and added mass force is:

$$\mathbf{f}_A = \frac{4}{3}\pi a^3 \rho_f \left( \left\langle \frac{D\mathbf{u}}{Dt} \right\rangle_{V_a} + \frac{1}{2} \left( \left\langle \frac{d\mathbf{u}}{dt} \right\rangle_{V_a} - \frac{d\mathbf{v}}{dt} \right) \right) \quad (5)$$

where the above  $\langle \dots \rangle_{V_a}$  denotes the volume average over the spherical particle. Putting together the two contributions, given by Equations (4) and (5), to the total force one obtain the equation of motion for a sphere,  $(4/3)\pi a^3 \rho_p d\mathbf{v}/dt = \mathbf{f}_D + \mathbf{f}_A$ , and keeping into account the Auton added mass correction for finite particle Reynolds numbers, i.e.,  $d\mathbf{u}/dt \rightarrow D\mathbf{u}/Dt$  [7], one obtain the phenomenological Faxén-corrected equation of motion:

$$\frac{d\mathbf{v}}{dt} = \frac{3 \rho_f}{\rho_f + 2 \rho_p} \left( \left\langle \frac{D\mathbf{u}}{Dt} \right\rangle_{V_a} + \frac{3\nu}{a^2} (\langle \mathbf{u} \rangle_{S_a} - \mathbf{v}) \right). \quad (6)$$

The above equation can be considered a generalization of Equation (2) and reduces to that equation in the limit  $D/\eta \rightarrow 0$ .

In [13] some first results obtained by numerical integration of Equation (6) are presented, along with preliminary comparison to experimental data. Here we show the behaviour of the Kaplan-Yorke dimension for the FC model. The Kaplan-Yorke dimension for the PP model was already discussed in [5, 16]. We recall that the phase space for the particle dynamics is  $(\mathbf{x}, \mathbf{v})$  thus we have 6 Lyapunov exponents. Due to the dissipative and chaotic nature of the dynamics, the phase-space distribution of particles evolves toward a dynamical (multi)fractal set. Fractal dimension of particle distribution can be measured by means of Kaplan-Yorke dimension [17] as  $d_\lambda = j + \sum_{i=1}^j \lambda_i / |\lambda_{j+1}|$  where  $j$  is the largest integer such that  $\sum_{i=1}^j \lambda_i > 0$ .

In Figure 4 it is shown the Kaplan-Yorke dimension as a function of  $\beta$  and  $St$  for the PP model (left panel) and the difference of  $D_{KY}$  for the FC and PP model (right panel). The present measurement is an useful quantitative indicator of where the finiteness of the particle play a larger role in the phase space dynamics. In [14] other quantitative results regarding the acceleration variance are presented and discussed.

### 3 Conclusions

In conclusion, we have shown that light/heavy point particles and light/heavy finite-size particles show highly non trivial statistics which is strongly affected by preferential concentration. In particular, we stress the importance for light

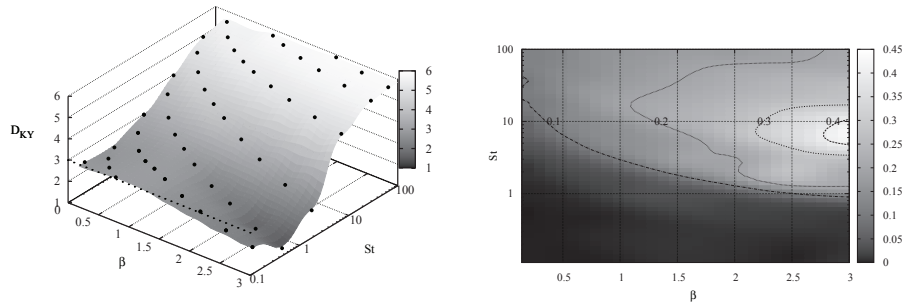


**Fig. 4.** The Kaplan-Yorke dimension  $D_{KY}$  vs.  $(\beta, St)$  for the PP model (left). The difference between the Kaplan-Yorke dimension as measured from the FC and the PP models,  $D_{KY}^{FC} - D_{KY}^{PP}$  (right). The phase space dynamics measured by KY dimension is not highly sensitive to the finiteness of the particle size.

particles to be concentrated inside vortex filaments, with strong consequent enhancement of the velocity intermittency along particle' trajectories. Such phenomenon may be of key importance for a proper stochastic modeling of light particle dispersion in turbulent fields. Experimental investigations of the Lagrangian properties of light particles would be of great value.

*Acknowledgments* We wish to acknowledge M. Bourgoïn, M. Cencini, A. Lanotte, J.-F. Pinton and R.Volk, for their contributions in former studies on numerical and experimental investigation of inertial particles.

## References

1. Frisch, U. *Turbulence: the legacy of A.N. Kolmogorov* (Cambridge University Press, Cambridge UK, 1995).
2. Mazzitelli, I.M., Lohse, D. and Toschi, F. "The effect of microbubbles on developed turbulence", *Phys Fluids* **15**, L5-L8 (2003).
3. Biferale, L., Boffetta, G., Celani, A., Devenish, B.J., Lanotte, A. and Toschi F., "Multifractal statistics of Lagrangian velocity and acceleration in turbulence", *Phys Rev Lett* **93** 064502 (2004).
4. Maxey, M.R. and Riley, J.J., "Equation of motion for a small rigid sphere in a nonuniform flow", *Phys. Fluids* **26** 883-889 (1983).
5. Calzavarini, E., Kerscher, M., Lohse, D. & Toschi, F., "Minkowski functionals: Characterizing particle and bubble clusters in turbulent flow", *J. Fluid Mech.* **607**, 13–24 (2008).
6. Calzavarini, E., Cencini, M., Lohse, D. & Toschi, F., "Quantifying turbulence-induced segregation of inertial particles" *Phys. Rev. Lett.* **101**, 084504 (2008).
7. Auton, T., Hunt, J. & Prud'homme, M. "The force exerted on a body in inviscid unsteady non-uniform rotational flow", *J. Fluid Mech.* **197**, 241–257 (1988).
8. Biferale, L., Boffetta, G., Celani, A., Lanotte, A., Toschi, F., "Particle trapping in three-dimensional fully developed turbulence" *Phys. Fluids* **17**, 021701 (2005).

9. Biferale, L. , Bodenschatz, E., Cencini, M., Lanotte, A., Ouellette, N., Toschi, F. and Xu, H., “Lagrangian structure functions in turbulence: A quantitative comparison between experiment and direct numerical simulation”, *Phys . Fluids* **20**, 065103 (2008).
10. Arneodo, A., Benzi, R. Berg, J., Biferale, L., Bodenschatz, E., Busse, A., Calzavarini, E., Castaing, B., Cencini, M. Chevillard, L., Fisher, R.T., Grauer, R. Homann, H., Lamb, D., Lanotte, A.S., Leveque, E., Luethi, B., Mann, J., Mordant, N., Mueller, W.-C., Ott, S., Ouellette, N.T., Pinton, J.-F., Pope, S.B., Roux, S.G., Toschi, F., Xu, H.,Yeung, P.K., “Universal intermittent properties of particle trajectories in highly turbulent flows”, *Phys. Rev. Lett* **100**, 254504 (2008).
11. Bec, J., Biferale, L., Cencini, M., Lanotte, A.S., Toschi, F., “Effects of vortex filaments on the velocity of tracers and heavy particles in turbulence” *Phys. Fluids* **18**, 081702 (2006).
12. Douady, S., Couder, Y., Brachet, M.E., “Direct observation of the intermittency of intense vorticity filaments in turbulence” *Phys. Rev. Lett.* **67** 983-986 (1991).
13. Calzavarini, E., Volk, R., Bourgoïn, M., L ev eque, E., Pinton, J.-F., Toschi, F., “Acceleration statistics of finite-sized particles in turbulent flow: the role of Fax en corrections”, **JFM in press**.
14. Calzavarini, E., Volk, R., Bourgoïn, M., L ev eque, E., Pinton, J.-F. and Toschi, F., “Effect of Fax en forces on acceleration statistics of material particles in turbulent flow”, proceeding of ETC12 in this same volume.
15. Gatignol, R. “The fax en formulae for a rigid particle in an unsteady non-uniform stokes flow” *J. M ecanique Theorique et Appliqu ee* **1**, 143–160 (1983).
16. Toschi F. and Bodenschatz E. “Lagrangian properties of particles in Turbulence” **Ann. Rev. Fluid Mech.** **41** 375-404 (2009).
17. Kaplan, J. L. and Yorke, J. A.in *Chaotic Behavior of Multidimensional Difference Equations*, Lecture Notes in Mathematics, eds. Peitgen, H.-O. and Walther, H.-O. (Springer, Berlin), **730**, 204227 (1979).